J. Fluid Mech. (1983), *vol.* 133, *pp.* 321–343
Printed in Great Britain

Double-diffusive plumes in unconfined and confined environments

By TREVOR J. McDOUGALL†
Research School of Earth Sciences, Australian National University,
GPO Box 4, Canberra, A.C.T.

(Received 27 July 1982 and in revised form 14 April 1983)

We address two aspects of the influence of double diffusion on convection from point buoyancy sources (plumes). First we consider double-diffusive convection acting in conjunction with buoyancy from an isolated source in an unconfined environment, and we study the problem of when fluxes of properties occur in the opposite direction to that of the initial buoyancy. A simple dimensional analysis is in good agreement with the experimental data for these 'counterbuoyant' fluxes of properties. Secondly, we consider a double-diffusive plume discharging into a confined environment. The plume now does not always reach the bottom (or top) of the confined environment, but can spread out into the environment at intermediate depths. Double-diffusive interfaces form, and we describe their development and the evolution of the density profile in the confined environment. A quantitative measure of the importance of double-diffusive convection in relation to the normal filling-box mechanism is obtained in the experiments by using the measured density profile, and this correlates well with a theoretically derived parameter B_ρ.

1. Introduction

Baines & Turner (1969) studied the processes that occur when a plume discharges into a confined environment. This situation has become known as a 'filling-box' experiment. Consider a dense plume entraining fluid from a box which is initially filled with a homogeneous fluid. When the plume reaches the bottom of the box, it spreads out horizontally and begins to fill the box from below. Plume fluid arriving later spreads out underneath this previous layer, and eventually a stable stratification is established in the environment. Baines & Turner derived the form of this stratification as a function of depth for the asymptotic regime as time approaches ∞. In this limit the density of the fluid at all depths below the source increases linearly with time. Germeles (1975) has presented a numerical model which successfully describes the unsteady development of the density structure in the tank before this asymptotic regime is reached. Manins (1979) has extended the Baines & Turner model to include the diffusion of density down the interior density gradient and also a diffusion boundary condition at the height of the source. Killworth & Turner (1982) have studied the filling-box situation with a plume that has a time-varying buoyancy flux. They showed that the resulting density profile in the box depends primarily on the maximum value of the imposed cyclical buoyancy flux.

In this paper we consider plumes in which the density contrast between the source fluid and the initial environment fluid is caused by two separate properties with

† Present address: Division of Oceanography, CSIRO, GPO Box 1538, Hobart, Tas. 7001. Australia.

different molecular diffusivities (e.g. heat and salt) which have opposing effects on the density difference between the source fluid and the environment. First we study the influence of double-diffusive convection on a plume which is discharging into an unconfined environment. That is, we concentrate on the influence of double-diffusive convection on the turbulent plume itself rather than on any property gradients which later develop in the environment. Turner & Chen (1974) performed related experiments using a zero buoyancy flux (i.e. where the initial densities of the 'plume' and environment fluid were equal) and we deal with the more general case where the buoyancy flux from the source is non-zero. That is, we examine the competing effects of the buoyancy from the source and double-diffusive convection. The buoyancy tends to produce a unidirectional plume whereas double-diffusive convection tends to produce both up and downward motions and fluxes of properties.

Secondly, we consider a double-diffusive plume entering a confined environment. This is the 'filling-box' geometry, and we examine a plume with two property contrasts which contribute to its excess density. The double-diffusive convection may be strong enough so that the plume splits into both an upgoing plume and a downgoing plume. In this case the box will 'fill' from both the bottom and the surface. This behaviour was demonstrated experimentally by Turner & Chen (1974). On the other hand, the buoyancy of the plume may outweigh the double-diffusive processes acting between the plume and the environment, and then we would expect its behaviour to be close to that of a single-component plume. The turbulence in the plume would then ensure that the influence of double-diffusive convection was negligible and the plume would fall to the bottom of the box and spread out horizontally. As the box fills in the normal 'filling-box' fashion, a stable density gradient forms in the environment with opposing gradients (in density units) of the two properties. Double-diffusive convection will now act on these gradients in the environment, causing an increase in the density of the fluid near the bottom of the box and a corresponding decrease of the density of the fluid in the upper part of the box. The plume then entrains fluid from the upper region of the box which is less dense owing to the double diffusion, and by the time the plume has fallen to near the bottom of the box it may be less dense than the fluid there. Consequently, it begins to spread out into the environment above this denser fluid. In this way the double-diffusive convection in the environment (rather than in the plume itself) creates a qualitative change to the normal filling-box mechanism, namely, the 'lift-off' of the plume fluid from the bottom of the tank. The density and property profiles in the box are also changed by this 'lift-off' process.

By comparing the strength of the two competing processes (double-diffusive convection and the filling-box mechanism), we derive a theoretical non-dimensional number B_ρ, the size of which indicates whether lift-off occurs or not. An experimentally determined overall measure of the effect of double-diffusive convection on the density profiles in the box also correlates well with B_ρ, and this confirms the relevance of B_ρ in determining the relative importance of the two competing processes.

There are several applications of this double-diffusive filling-box process. The phenomenon of 'rollover' in liquid natural gas (LNG) storage containers occurs because of stratification which develops in the tanks during refilling. The inflowing LNG is often at a different temperature and has a different composition (proportion of various gases) to the existing tank fluid and it is added near the top of the tank in some cases and near the bottom in other cases. Sarsten (1972) discusses the rollover problem and gives data on the dangerously high pressures that occurred in a particular case. In order to gauge the importance of double-diffusive convection in

this LNG storage refilling problem, it will be necessary to obtain quantitative data on the double-diffusive fluxes of heat and the fastest-diffusing liquid component of the LNG across a sharp interface.

A second application is to the production of warm saline bottom water in the world's ocean by the outflow of very dense warm saline water from marginal seas. There is mounting evidence (Brass *et al.* 1982) that the ocean bottom water was 15 °C about 70 million years ago, and Peterson (1982) has developed a model of this process which emphasizes the influences of multiple sources of buoyancy on the resulting property profiles in the ocean. The sources of dense water from the marginal seas were both warmer and saltier than the surrounding sea water, and so we expect double diffusion to be important.

Another application of this work is to the formation of massive sulphide deposits. Turner & Gustafson (1978) first raised the importance of a filling-box geometry when a dense gravity current of hot saline ore solution fills a depression on the sea floor (their figure 18). Again the source is both relatively warm and salty and the results of this paper will be appropriate.

This work is also applicable to convection in magma chambers. Huppert & Sparks (1980) have recently demonstrated the importance of double-diffusive convection in a replenished magma chamber. The relatively large flux of heat which occurs by double-diffusive convection (compared with the heat fluxes due to conduction through the surrounding rocks) coupled with the crystallization of rocks in the lower part of a magma chamber, can cause a rapid and unexpected 'rollover' in the chamber. More recently, Turner & Gustafson (1981) have discussed the fluid-dynamic implications of cooling and crystallization at the sidewall of a magma chamber (and a laboratory tank). Gradients of properties are established in the environment by the filling-box mechanism, although the buoyancy source is now a plane wall (or a number of such walls). Recent laboratory experiments by Leitch (1982 personal communication) have shown that this change of geometry causes a number of additional and complicating features, but our results with a point-source double-diffusive plume in a confined environment should give valuable insights in understanding these more complicated experiments.

2. The influence of double-diffusive convection on turbulent plumes

In this section we consider a double-diffusive plume discharging into an effectively infinite environment. The term 'double-diffusive plume' is taken to mean a source of buoyancy which is caused by two different properties which have different molecular diffusivities and opposing effects on the density of the source fluid. The component with the larger molecular diffusivity κ_T we call T and that with the smaller molecular diffusivity κ_S we call S.

Figure 1 shows a slightly denser salt solution discharging into a sugar solution. This discharge flow rate was quite small, and little horizontal momentum was given to the plume. The bunches of thin rising streamers of fluid are typical of this form of double-diffusive convection.

2.1. *The different experimental configurations*

In this discussion we consider heat and salt as the two properties which contribute to the fluid density, and there are four different source configurations. These include relatively warm and salty sources or the opposite case of relatively cool and fresh sources, and in both of these cases the incoming plume fluid can be either more dense

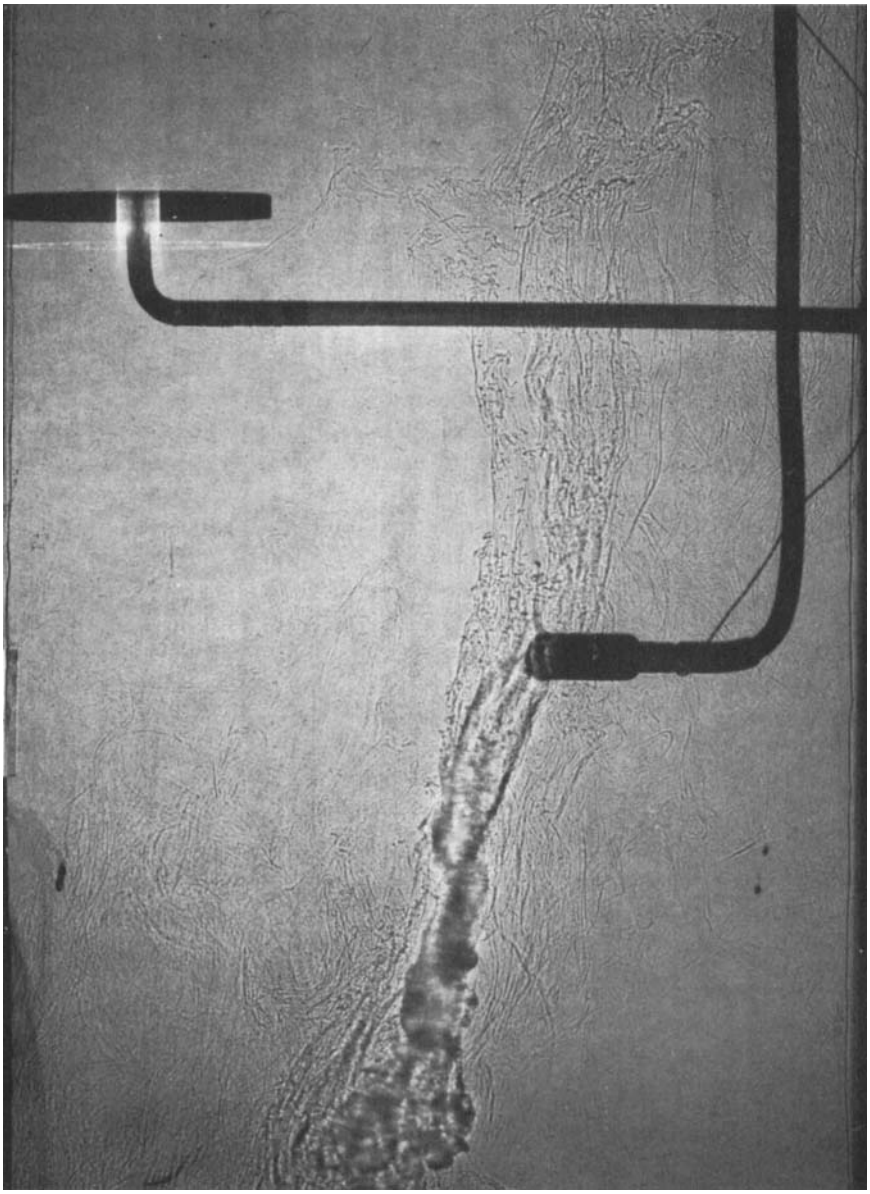

FIGURE 1. A photograph of slightly denser ($\delta\rho \approx 10^{-3}$ g cm^{-3}) salt solution flowing into sugar solution ($\alpha\Delta T \approx \beta\Delta S \approx 0.1$) at a flow rate of 0.3 cm^3 s^{-1}. Note that at this small flow rate very little horizontal momentum is given to the plume.

or less dense than the environment. In experiments with vertical initial plume motion we observed large oscillations in the double-diffusive plume. These oscillations were caused by the interaction of the main vertical motion of the plume with those fluid elements that had had the sense of their buoyancy reversed by double-diffusive convection and had begun to move in the opposite vertical direction to that of the main plume. These oscillations bear some resemblance to those described by Turner (1966) for vertical plumes with reversing buoyancy; that is, where the buoyancy reverses when the plume fluid is greatly diluted by mixing with the environmental fluid. We wished to avoid these oscillations in our experiments and so we used a

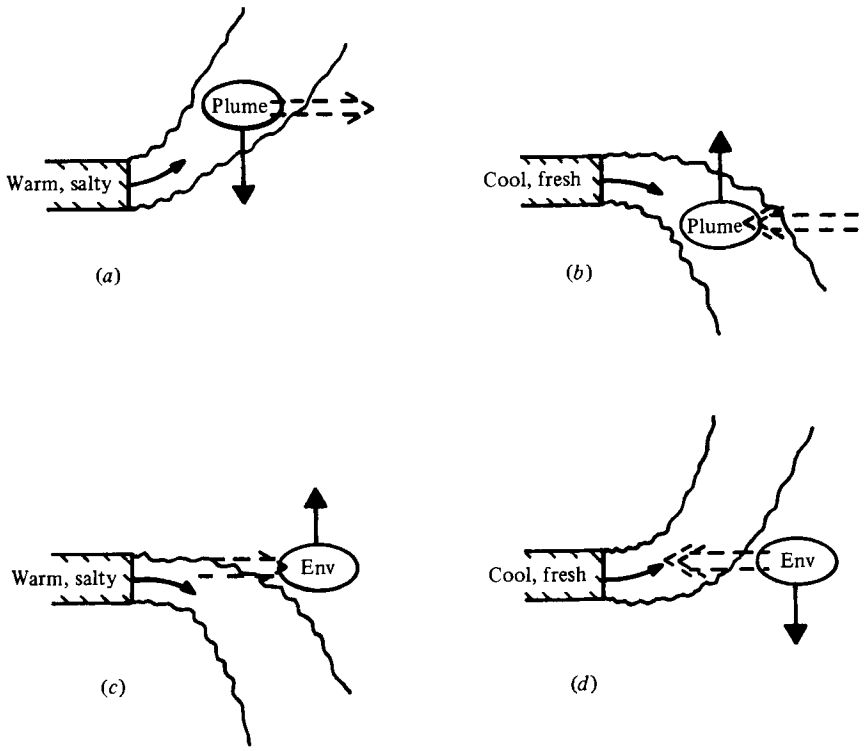

FIGURE 2. Sketches showing the four combinations of double-diffusive plumes entering a homogeneous environment. The source fluid can be either warmer and saltier than the environment (cases (*a*) and (*c*)) or cooler and fresher (cases (*b*) and (*d*)). The source fluid can be either less dense than the environment (cases (*a*) and (*d*)) or more dense (cases (*b*) and (*c*)). The dashed arrows show the direction of the heat flux between the plume and the environment.

horizontal nozzle which gave the plume fluid a little horizontal momentum. Vertical motion was always observed to dominate the flow at just a few nozzle diameters from the source, and so we do not think that the horizontal momentum from the source materially affected our results.

Consider now a parcel argument based on the assumption that, even though the plume is rising due to its buoyancy, it can still exchange heat with the environment. Consider a parcel of warm salty plume fluid as in figure 2(*a*) (the parcel is circled and labelled 'plume') which transfers some heat to the environment. We assume for simplicity that the flux of salt is insignificant. With a sufficiently large heat flux, the parcel of plume fluid will find that it is now more dense than the environment and may begin to fall. Some of the environment fluid near the plume will have gained heat, so it will begin to rise. Figure 2(*b*) is in a sense a mirror image of figure 2(*a*). The cool, fresh plume fluid is now more dense than the environment and its buoyancy causes it to fall. The transfer of heat from the environment into a parcel of the plume fluid will tend to make the plume fluid rise (as shown in figure 2*b*). The environment fluid from which the heat came will tend to fall.

The configuration in figures 2(*c*), (*d*) can also lead to vertical convection motion in the opposite direction to that of the initial vertical motion of the plume. Consider the case of a relatively dense, warm salty source fluid, shown in figure 2(*c*). When a parcel of plume fluid exchanges heat (but not salt) with the environment, the plume parcel itself becomes cooler and so has a greater tendency to fall in the direction

of the initial motion of the plume as a whole. On the other hand, the environment fluid that has received this heat is now less dense than its surroundings and so tends to rise. In an exactly analogous manner, a small parcel of the environment fluid in figure 2(*d*) tends to fall because it has cooled by transferring heat to the plume.

The above simple 'parcel arguments' are inevitably highly simplified but they are useful in distinguishing between the four different cases in figure 2.

2.2. *Dimensional analysis*

We concentrate on the double-diffusive plume configuration shown in figure 2(*a*). Let the volume flow rate from the source be Q. The temperature difference between the source fluid and the environment is ΔT and the corresponding difference in the S-concentration is ΔS. We wish to determine the dimensionless parameters that are important in setting the downward flux of heat, that is, the 'counterbuoyancy' flux of heat, which we shall label F_T^c. We express the general functional relationship between all the physical variables of the system as

$$f(g\alpha F_T^c, F_0, g\frac{\Delta\rho}{\rho_0}, g\alpha\Delta T, \nu, \kappa_T, \kappa_S) = 0, \tag{1}$$

where g is the gravitational acceleration, ν the kinematic viscosity, α is the expansion coefficient for the property T, $\Delta\rho$ is the density difference between the plume and the environment and F_0 is the buoyancy flux at the source, $Qg(\Delta\rho/\rho_0)$. We assume that it is primarily the diffusion of heat which produces the reversal of buoyancy of some of the plume fluid, as discussed in the parcel argument of figure 2(*a*). This assumption means that the molecular diffusivity κ_S of salt is not important, although the vertical *motion* which is caused by the molecular diffusion of heat may well lead to a significant downward flux of salt as well as heat. The double-diffusive flux of density across the edge of a parcel of plume fluid is proportional to $\kappa_T\alpha\Delta T$ divided by an appropriate distance scale over which diffusion occurs. This diffusion lengthscale presumably depends on the level of turbulent activity in the plume and on the Prandtl number ν/κ_T. We do not have a good estimate of this lengthscale and so we merely multiply the $g\alpha\Delta T$ term in (1) by κ_T and regard this combination as being proportional to the sideways flux of heat out of the plume. So long as the unknown lengthscale depends only on the other parameters that are retained in the dimensional analysis, this procedure is valid and leads to

$$f(g\alpha F_T^c, F_0, \kappa_T g\alpha\Delta T, g\frac{\Delta\rho}{\rho_0}, \frac{\nu}{\kappa_T}, \kappa_T) = 0. \tag{2}$$

The term $\kappa_T g\alpha\Delta T$ represents the ability of double-diffusive convection to cool the plume. In order for a parcel of plume fluid to sink (see figure 2*a*) it must be cooled sufficiently to overcome the density difference between the plume and the environment, and for this reason the $g\Delta\rho/\rho_0$ term must be retained as a variable in (2). The last two terms of (2) can be regarded as constant in any particular experiment, and this expression can then be rearranged to give

$$\begin{aligned} g\alpha F_T^c &= \frac{F_0^{\frac{1}{2}}}{(g\Delta\rho/\rho_0)^{\frac{1}{2}}}(\kappa_T g\alpha\Delta T)^{\frac{5}{6}} f\left(\frac{F_0 g\Delta\rho/\rho_0}{(\kappa_T g\alpha\Delta T)^{\frac{5}{3}}}\right) \\ &= Q^{\frac{1}{2}}(\kappa_T g\alpha\Delta T)^{\frac{5}{6}} f\left(\frac{F_0 g\Delta\rho/\rho_0}{(\kappa_T g\alpha\Delta T)^{\frac{5}{3}}}\right). \end{aligned} \tag{3}$$

We expect from the experiments of Turner & Chen (1974) that, when $\Delta\rho \approx 0$, $g\alpha F_T^c$ will be insensitive to small changes in $\Delta\rho$. The form of the expression (3) was chosen

with this in mind so that, as $\Delta\rho \to 0$, f can remain finite. We adopt the shorthand notations

$$\mathscr{H} \equiv \frac{g\alpha F_T^c}{Q^{\frac{1}{2}}(\kappa_T g\alpha\Delta T)^{\frac{5}{6}}}, \tag{4}$$

$$\mathscr{R} \equiv \frac{F_0 g\Delta\rho/\rho_0}{(\kappa_T g\alpha\Delta T)^{\frac{5}{3}}}, \tag{5}$$

and (3) is then simply

$$\mathscr{H} = f(\mathscr{R}). \tag{6}$$

The 'counterbuoyant' flux of heat in the case of figure 2(*c*) (and 2*d*) should also follow the same functional form (6). In summary, this result, based on dimensional analysis, has been obtained by neglecting the influence of κ_S for constant molecular properties ν and κ_T and by the grouping of the temperature difference scale ΔT, which is available to drive counterbuoyancy motion, with the molecular diffusivity of heat κ_T.

2.3. *Experimental results*

Experiments were conducted in the configurations of both figures 2(*a*) and (*c*) with warm saline plume water entering horizontally at mid-depth into a tank of relatively cool fresh water. The tank had a removable horizontal barrier (as described in McDougall 1981) which could be inserted at mid-depth between the upper and lower halves of the tank. Care was taken to have the initial temperature of the water in the tank very close to room temperature. The front and back faces of the tank were double perspex walls separated by a sealed 6 mm airgap and the sides and top of the tank were covered with polystyrene sheet. In this way the loss or gain of heat to the room was kept acceptably small. The temperature of the incoming source fluid was measured immediately before entering the tank by a thermistor in the nozzle. The procedure used in the experiments was to allow the plume fluid to flow into the tank for a set time (between 3 and 15 minutes) and then to turn off the source and insert the barrier. When the barrier was in place, the upper and lower layers were thoroughly stirred and the properties (temperature and salinity) of the layers were measured, The salinities were determined by taking samples from the layers and using a conductivity bridge (Beckman model RC-18A). A 35 m length of fine copper resistance wire was wound on each of two perspex tube frames and they were placed in the centre of each layer. The wires' change of resistance with temperature was used in two simple Wheatstone bridges to determine the temperatures of the layers to an accuracy of ± 0.002 °C. When expressed in density units, the salinity measurements had error bars only four times those of temperature.

In these experiments the volume flow rate from the source was varied from 1 to 9 cm^3 s^{-1} and the density difference between the source and the environment ranged from 10^{-4} to 10^{-3} g cm^{-3}. The source Reynolds number was always greater than 200 and the flow was observed to become unstable within a few nozzle diameters downstream. The temperature difference between the source and the environment was within the range 8 to 12 °C, and as the density differences were small the nonlinearity of the equation of state was quite important in the determination of $\Delta\rho$. The equation of state of Ruddick & Shirtcliffe (1979) was used to evaluate density and to obtain the expansion coefficients α and β. Because turbulent mixing occurs near the source, the most relevant measure of an effective density difference is probably $(\alpha F_T - \beta F_S)/Q$, where α and β are evaluated at the environment values of T and S, and F_T and F_S are the fluxes of T and S from the source (referred to the environment temperature and salinity). This effective density difference was

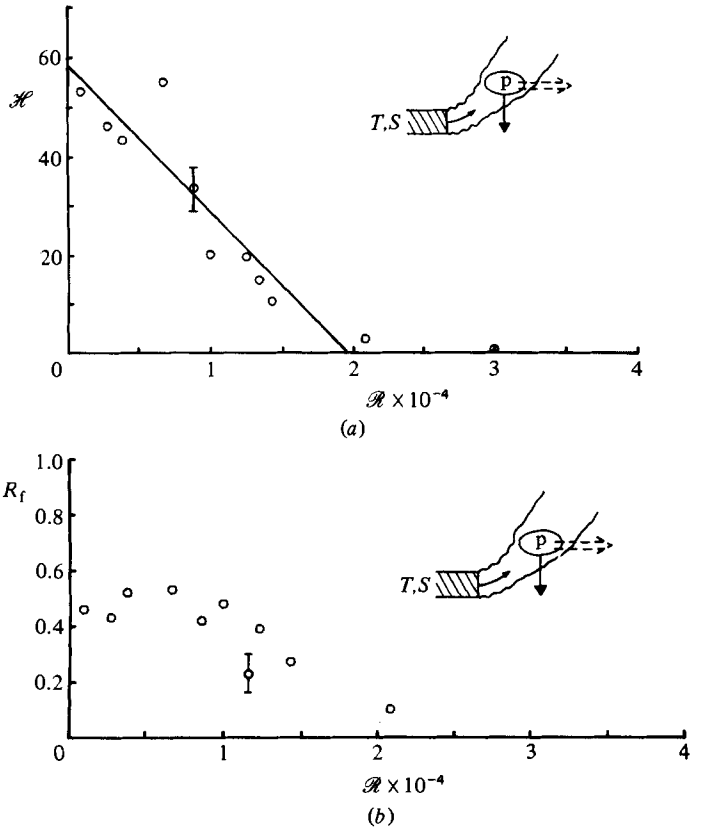

FIGURE 3. (*a*) The nondimensional counterbuoyant flux of heat $\mathscr{H}$ in the case of figure 2(*a*) as a function of the parameter $\mathscr{R}$, which represents the relative strengths of the buoyancy flux and the double-diffusive convection. (*b*) The buoyancy-flux ratio $R_f \equiv \alpha F_T^c / \beta F_S^c$ for the case of figure 2(*a*) plotted against $\mathscr{R}$.

significantly different from the actual density difference between the source and the environment, and the practice we adopted to evaluate $\Delta\rho$ was to take the average of these two density differences.

Figure 3(*a*) shows the counterbuoyancy heat flux in the configuration of figure 2(*a*). This heat flux is non-dimensionalized as in (4) and is plotted against $\mathscr{R}$. For given values of g and κ_T, the abscissa $\mathscr{R}$ in figure 3 is proportional to $F_0 \Delta\rho \Delta T^{-\frac{5}{3}}$, where $\Delta\rho$ is the density difference between the source and the environment, and for large values of $\mathscr{R}$ the double-diffusive nature of the plume is unimportant in relation to its buoyancy, and $\mathscr{H} = 0$. A large buoyancy flux F_0 at the source or a large density difference $\Delta\rho$ there will enhance the ordinary buoyant plume behaviour, as will a small ΔT. The straight line drawn on figure 3(*a*) is not proposed as a close fit to the data but rather to emphasize the fact that the counterbuoyant flux of heat goes to zero for values of $\mathscr{R}$ greater than about 2×10^4 and that for smaller values of $\mathscr{R}$ there is an increasing flux which is maximized at $\mathscr{R}$ equal to zero. The buoyancy flux ratio R_f is the downward flux of heat divided by the downward flux of salt (both expressed in density units). Figure 3(*b*) shows the experimental results for R_f. Typical values are near $R_f \approx 0.5$, but there is a tendency for R_f to decrease at larger $\mathscr{R}$. The error bars increase at the large values of $\mathscr{R}$ because the counterbuoyant fluxes of both heat and salt are small.

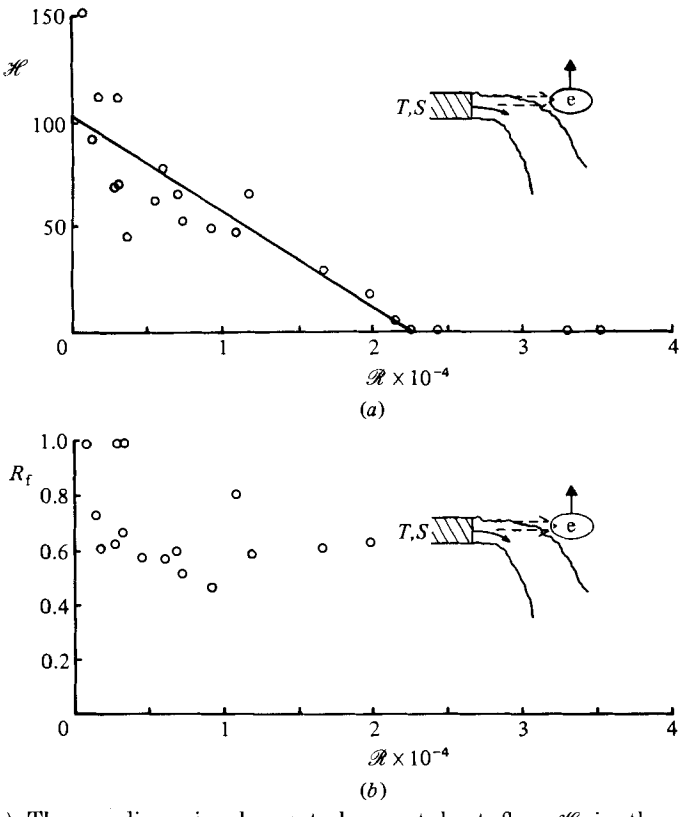

FIGURE 4. (*a*) The nondimensional counterbuoyant heat flux $\mathscr{H}$ in the case of figure 2(*c*) as a function of $\mathscr{R}$. (*b*) The buoyancy-flux ratio $R_f \equiv \beta F_S^c / \alpha F_T^c$ for the case of figure 2(*c*) plotted against $\mathscr{R}$.

The corresponding results for the configuration of figure 2(*c*) are shown in figures 4(*a*, *b*). Once again the double-diffusive 'counterbuoyancy' fluxes cease for $\mathscr{R} \gtrsim 2 \times 10^4$. There is more scatter in the data in this case, but a general increase in $\mathscr{H}$ is readily apparent as $\mathscr{R}$ decreases. Note that the typical heat fluxes are larger by a factor of two in this case; however, the counterbuoyant fluxes of buoyancy, equal to $g\alpha F_T^c(1-R_f)$ in the case of figure 2(*c*) and $g\alpha F_T^c(R_f^{-1}-1)$ in the case of figure 2(*a*), are similar.

3. The double-diffusive filling-box process

3.1. *The relative importance of double-diffusive convection and the filling-box process*

We consider a negatively buoyant plume flowing into a confined environment from above. The plume is assumed to be ideal, in the sense that its volume flow rate at the source is zero. The flux of buoyancy in the plume is due to two properties which have different diffusivities. If these two properties have opposite effects on the density of the source then the stable density gradient in the box will exhibit double-diffusive convection and density will be transported against the density gradient, thereby increasing the density of the lowermost region of the box. If this double-diffusive convection is sufficiently strong, the plume fluid will no longer be dense enough to

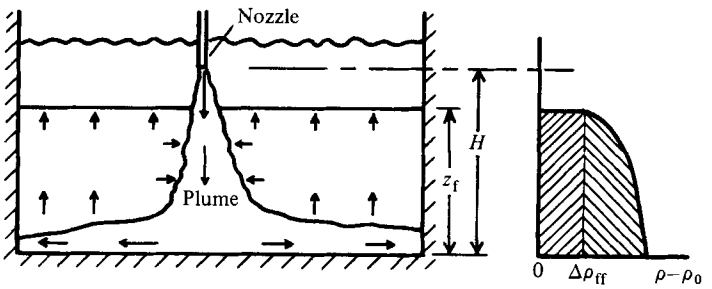

FIGURE 5. Sketch of a source of buoyancy discharging into a confined environment. The source is a height H above the bottom of the tank, and the height of the first front is z_f. The horizontal area of the tank is A. The density profile of the environment fluid is sketched when $z_f = 0.82H$ and the two shaded areas in the density profile are equal.

flow out along the bottom of the box, but instead will flow out into the interior at an intermediate depth. We now consider under what conditions this behaviour is expected to occur, and in the following we discuss the flow in terms of the heat–salt system set up in the diffusive sense. We emphasize that in this section of the paper we are not considering double-diffusive convection in the plume itself as we did in §2. The double-diffusive convection with which we are concerned in this section occurs in the environment and property gradients there are initially established by the filling-box mechanism.

The density difference ($\Delta\rho_{ff}$) across the first front is simply the density difference between a plume and its environment at a distance H (the height of the source above the bottom of the box) from a source of buoyancy F_0 (see figure 5). This is given by

$$\frac{g}{\rho_0}\Delta\rho_{ff} = 8.67 F_0^{\frac{2}{3}} H^{-\frac{5}{3}} \tag{7}$$

(Turner 1973), where we have used a value of 0.1 for the entrainment constant of an axisymmetric plume. Now we need to specify the double-diffusive character of the source of the buoyancy.

We define the density anomaly ratio R_ρ by $R_\rho = \beta\Delta S/\alpha\Delta T$ (for a diffusive interface), where ΔS and ΔT are the magnitudes of the differences in salinity and temperature between the source fluid and the homogeneous environment fluid. This definition suffices for laboratory experiments, but for the ideal sources of buoyancy which we are considering in this section, R_ρ should really be defined using the ratio of the fluxes of salt and heat (referred to the environment salinity and temperature) from the source (in density units). The temperature difference across the first front (in the absence of double-diffusive convection) is given by $\alpha\Delta T_{ff} = \Delta\rho_{ff}/\rho_0(R_\rho - 1)$. Using the formula given by Huppert (1971) for the heat flux F_h across a diffusive interface, we have the following expression for the flux of heat across the first front:

$$\left.\frac{\alpha F_h}{\rho_0 C_p}\right|_{ff} = 0.323\left(\frac{g\kappa_T^2}{\nu}\right)^{\frac{1}{3}} \frac{(\alpha\Delta T_{ff})^{\frac{4}{3}}}{R_\rho^2}, \tag{8}$$

where C_p is the specific heat of the fluid and ν is the kinematic viscosity. This flux of heat and the associated double-diffusive flux of salt will cause the fluid below the first front to increase in density at an average rate $\dot{\rho}_{dd}$ (the dd subscript meaning double diffusion) given by

$$z_f\dot{\rho}_{dd} = \rho_0 \left.\frac{\alpha F_h}{\rho_0 C_p}\right|_{ff} (1 - R_f), \tag{9}$$

where R_f is the flux ratio of the double-diffusive convection and z_f is the depth of the first front above the bottom of the tank. This rate of change of density beneath the first front is to be compared with the average rate of change of density caused by the filling-box process, namely $\dot{\rho}_{fb}$, given by

$$z_f \dot{\rho}_{fb} = \frac{\rho_0 F_0}{gA}, \tag{10}$$

where g is the gravitational acceleration and A is the (uniform) horizontal area of the box. The ratio of these two rates of change of density gives the required indication of the strength of (i) the double-diffusive convection in causing a density increase below the first front compared with (ii) that of the filling-box process. This non-dimensional parameter we call B_ρ, and from the above equations (7)–(10) it is given by

$$B_\rho \equiv \frac{\dot{\rho}_{dd}}{\dot{\rho}_{fb}} = \frac{0.34}{R_\rho^2} \frac{A}{H^{\frac{20}{9}}} \frac{1-R_f}{F_0^{\frac{1}{3}}(R_\rho - 1)^{\frac{4}{3}}} \quad \text{heat–salt diffusive,} \tag{11a}$$

where the constant term has units of cm s^{-1} and is in fact equal to $5.75\kappa_T^{\frac{2}{3}} \nu^{-\frac{1}{3}}$. In (11*b–d*) below we simply use the dimensional constant in units of cm s^{-1}. The corresponding expression for B_ρ for the sugar–salt diffusive case is

$$B_\rho = \frac{0.077}{R_\rho^{12.6}} \frac{A}{H^{\frac{20}{9}}} \frac{1-R_f}{F_0^{\frac{1}{3}}(R_\rho - 1)^{\frac{4}{3}}} \quad \text{sugar–salt diffusive,} \tag{11b}$$

where we have used the power law of Shirtcliffe (1973) for the salt flux. For the heat–salt finger case we have used the following fit to the data of Schmitt (1979) for the salt flux F_S, $\beta F_S = (0.134/R_\rho^{\frac{1}{2}})(g\kappa_T)^{\frac{1}{3}}(\beta \Delta S)^{\frac{4}{3}}$, to obtain

$$B_\rho = \frac{0.268}{R_\rho^{\frac{1}{2}}} \frac{A}{H^{\frac{20}{9}}} \frac{1-R_f}{F_0^{\frac{1}{3}}(R_\rho - 1)^{\frac{4}{3}}} \quad \text{heat–salt finger} \tag{11c}$$

(R_ρ is $\alpha \Delta T / \beta \Delta S$ for the finger case). For the sugar–salt finger case the sugar-flux power law of Griffiths & Ruddick (1980) leads to

$$B_\rho = \frac{0.01}{R_\rho^6} \frac{A}{H^{\frac{20}{9}}} \frac{1-R_f}{F_0^{\frac{1}{3}}(R_\rho - 1)^{\frac{4}{3}}} \quad \text{sugar–salt finger.} \tag{11d}$$

Note that these four expressions each have the same dependence on the flux ratio R_f, the buoyancy flux F_0, the geometrical factors A and H, and the $R_\rho - 1$ term. We see that B_ρ is not very sensitively dependent on F_0 but increases dramatically when R_ρ is close to unity due mainly to the $(R_\rho - 1)^{-\frac{4}{3}}$ factor.

We have explained how the double-diffusive convection increases the density of the fluid below the first front, but it will also decrease the density of the fluid above the first front. The extent to which this occurs will depend on the volume of fluid above the first front. This effect will increase the influence of the double-diffusive convection on the plume behaviour because the plume will entrain less dense fluid initially (from above the first front), later to find itself surrounded by denser fluid below the first front. Another effect of active double-diffusive convection is to cause the stratified region below the first front to break up into a series of well-mixed layers and sharp density interfaces.

The non-dimensional number B_ρ gives an estimate of the relative importance of the two processes at work, namely double-diffusive convection and the filling-box mechanism. A readily observed feature of an experiment is whether the plume fluid which flows into the environment ever 'lifts off' the bottom of the tank. While this is an easily observed qualitative feature of the flow, a more quantitative measure

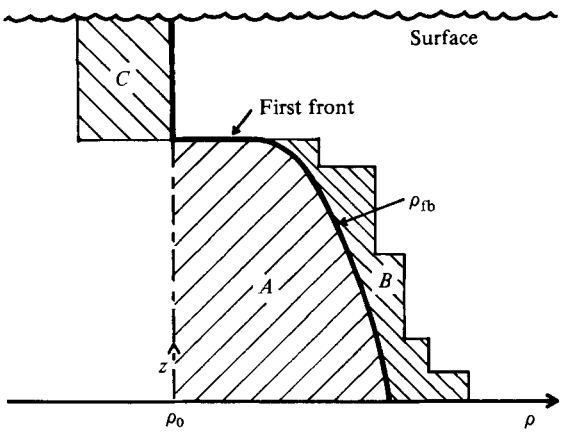

FIGURE 6. Sketch of the density profile observed in a double-diffusive filling-box experiment (stepped profile) and the smooth density profile which would be caused by the filling-box process alone.

of the importance of double-diffusive convection in an experiment is given by the following expression, which we call D_ρ:

$$D_\rho \equiv \frac{\frac{1}{2}\int_0^{\text{surface}} |\rho - \rho_{fb}|\, dz}{\int_0^{\text{surface}} (\rho - \rho_0)\, dz}. \tag{12}$$

This parameter represents the extent to which double-diffusive convection has redistributed the density in the vertical as a proportion of the total input of buoyancy from the plume. The density ρ_{fb} in (12) is the density as a function of depth which would be created by a flux of buoyancy F_0 purely by the filling-box process. This is readily calculated by the theory of Baines & Turner (1969) for the asymptotic case where the plume has been flowing for some time. Figure 6 shows a sketch of $\rho_{fb}(z)$ and a typical density profile which we observe in our experiments. The parameter D_ρ is defined in terms of the areas in figure 6 by $\frac{1}{2}(B+C)/A$.

Before moving on to the experimental results, we discuss a measure of the 'filling-box timescale', which we label t_{fb}. Baines & Turner (1969) derive a formula (their equation (6)) for the time t taken for the first front to reach a height z_f, and using a value of 0.1 for the entrainment coefficient of an axisymmetric plume, this equation becomes

$$t = 8.19 A F_0^{-\frac{1}{3}} [(H - z_f)^{-\frac{2}{3}} - H^{-\frac{2}{3}}]. \tag{13}$$

We propose that a typical filling-box timescale be the time taken for the average density excess below the first front to be twice the density step across the first front, $\Delta\rho_{ff}$, given by (7). This is illustrated in the density profile of figure 5. The average excess density below the first front is given by $(\rho_0/g) F_0 t/HA$. Putting this equal to $2\Delta\rho_{ff}$ and using (7) and (13), we find that this occurs when $z_f = 0.82H$ at the typical filling-box timescale t_{fb} given by

$$t_{fb} = 17.3 A F_0^{-\frac{1}{3}} H^{\frac{2}{3}}. \tag{14}$$

If the volume flow rate Q from the source is not zero then there is also a much larger timescale given by HA/Q. When a source has been flowing for this length of time, the total volume added from the source is equal to the volume of the confined environment below the nozzle. A non-zero Q implies that after some time the 'first

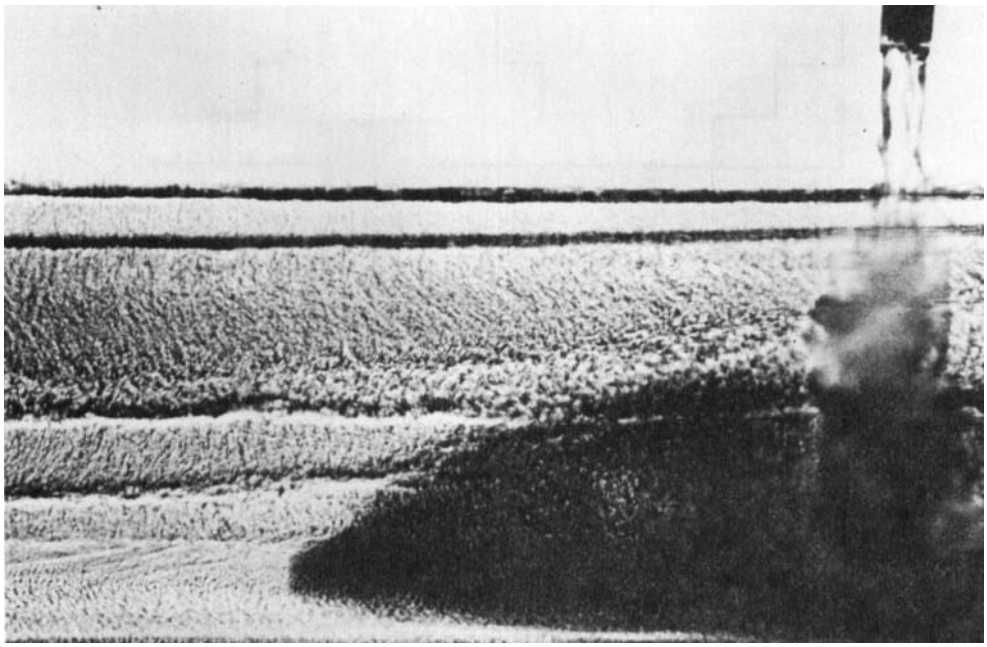

FIGURE 7. A shadowgraph of the central part of the tank. The nozzle is 25 cm above the floor of the tank. The volume flow rate from the source is 3 $cm^3\ s^{-1}$, the density-anomaly ratio R_ρ is 1.054 in the 'diffusive' sense, with a source of sugar going into a tank of salt solution. The darker region marks the movement of dye put into the plume a short time before the photograph was taken. The photograph was taken 3.5 h after the start of the experiment. The typical filling-box timescale t_{fb} for this experiment was 3.2 h.

front' rises past the nozzle, and we avoid this complication in this paper by considering ideal buoyancy sources with $Q \to 0$. In practice this means that we perform experiments for times much less than HA/Q.

3.2. *Laboratory experiments and their interpretation*

These experiments were performed in a large glass tank 2 m long by 0.6 m wide and 0.6 m high. The source of buoyancy was placed in the middle of the horizontal area of the tank and 25 cm above the bottom. A general characteristic of double-diffusive convection is the formation of well-mixed layers and sharp interfaces, and these features were often evident in our experiments. Figure 7 shows several such interfaces. The darker region of the photograph (lower right-hand side) is due to dye which was added to the plume about five minutes before the photograph was taken. This dark region then marks the levels at which recent plume fluid has spread out. In contrast with the ordinary filling-box behaviour, the plume fluid in figure 7 does not spread out along the bottom of the box, but rather it interacts directly with the environment over a range of depths.

3.2.1. *A simple physical description of 'lift-off'*

Consider the diffusive regime with the solutes sugar and salt. Prior to 'lift-off' there are gradients of salt T, sugar S and density ρ near the bottom of the tank similar to those shown in figure 8(*a*) by the solid lines. Double-diffusive convection across the lowermost interface of figure 8(*a*) transports T and S down their gradients, but

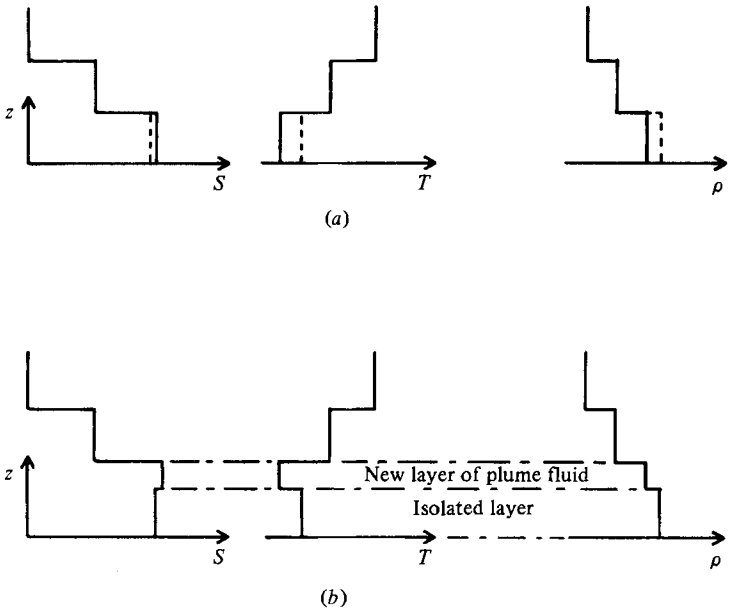

FIGURE 8. Sketches of the initial 'lift-off' process in the sugar (S)–salt (T) diffusive case. The dashed lines in (a) show the effects of double-diffusive convection on the lowest layer. In (b) is shown the most-recent plume fluid flowing out above an 'isolated' layer.

density is transported against its gradient. The properties of the lowest layer move to those shown by the dashed lines in figure 8 (a). The newly arrived plume fluid, with T, S and ρ similar to the lowest-layer values prior to double-diffusive convection, will now tend to spread horizontally above this lowest layer. The property profiles are now as shown in figure 8 (b). An interesting change has now occurred in the nature of the interface at the top of the 'isolated layer'. The properties T and S are now distributed in the *finger* sense across this interface.

3.2.2. *The double-diffusive nature of the layer and interface structure*

We now present a selection of the detailed measurements of T, S and ρ during the experiments. The experiments were conducted in both the diffusive and finger regimes with both the sugar–salt and the heat–salt property pairs. Figure 9 (a) shows the profiles of αT, βS and density as a function of depth, $5\frac{1}{2}$ h after the start of a sugar–salt diffusive experiment with $R_\rho = 1.0543$ and $B_\rho = 0.048$. This is the same experiment shown in the photograph of figure 7, which was taken at an earlier time. The profiles were drawn by taking into account the visual observations from the shadowgraphs that the tank was filled with a series of well-mixed layers and sharp interfaces. Samples were withdrawn from each layer and later analysed for density and conductivity to determine the three properties αT, βS and σ. The layered nature of the profiles of figure 9 (a) is then due to our reconstruction of the profiles on the basis of the observed mixed layers, rather than of any measured detailed vertical structure. Note the similarity of the lower part of these profiles with those sketched in figure 8 (b). The lowermost interface is stratified in the finger sense, which indicates that the most recently arrived plume fluid is flowing into the box above this level. From our experiments, such isolated layers do not remain isolated indefinitely. There are two opposing processes at work here and it is not possible to say unambiguously which process will dominate in general. On the one hand, the finger double-diffusive

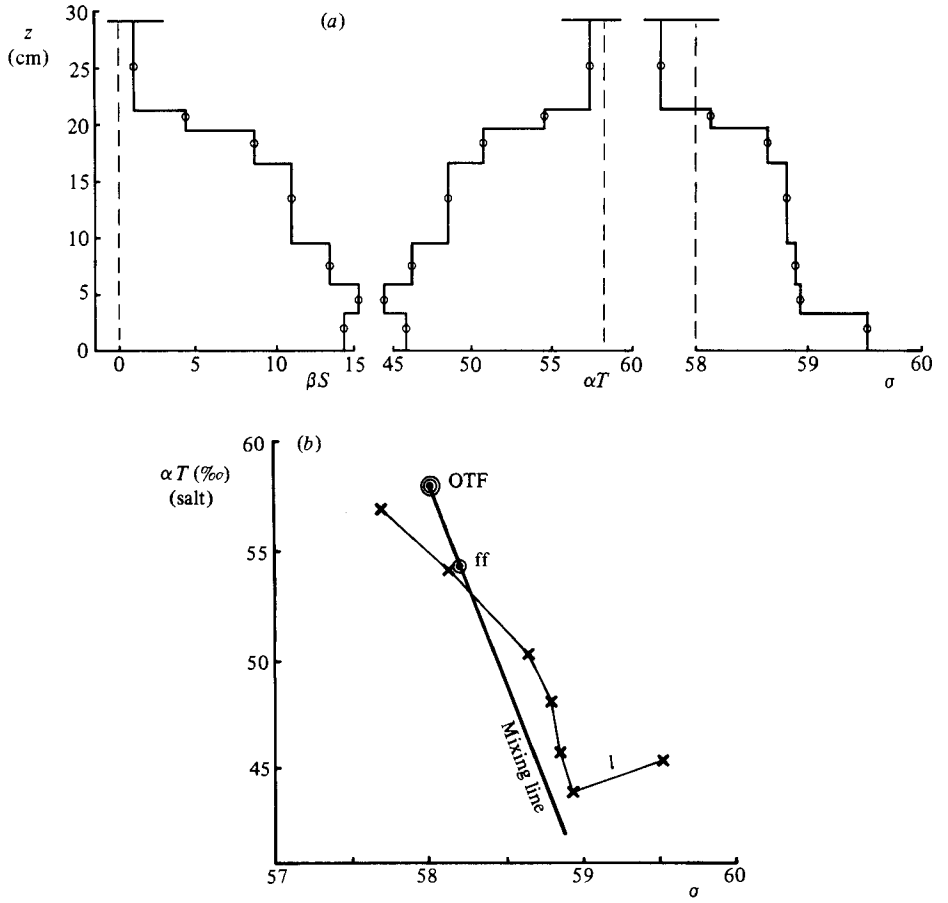

FIGURE 9. (*a*) Profiles of properties measured at $5\frac{1}{2}$ h after the start of a diffusive sugar–salt experiment (i.e. denser sugar plume discharging into a less-dense saline environment). The density-anomaly ratio R_ρ was 1.0543 and B_ρ was 0.048. The values of βS, αT and σ of the tank fluid before the experiment began are shown by the dashed lines. The symbol σ is defined by $\sigma \equiv (\rho - 1) \times 10^3$, where ρ is the density in g cm^{-3}. The typical filling-box timescale t_{fb} was 3.2 h. (*b*) Graph of salt content versus density for the sugar–salt diffusive experiment with $R_\rho = 1.0543$. The point labelled 'ff' represents the theoretically derived properties immediately below the first front if double-diffusive convection were absent. The symbols 'OTF' mean original tank fluid.

convection across the lowermost interface makes the lowest layer denser and so tends to preserve its identity. On the other hand, the continual action of the plume in the filling-box geometry tends to increase the density of the plume fluid which flows out into the environment, so tending to equalize the densities across the lowermost interface.

Figure 9(*b*) is another way of plotting this same data which emphasizes the double-diffusive nature of these processes. On this diagram we plot one property against another (in this case we plot αT against density as $\sigma \equiv (\rho - 1) \times 10^3$) rather than against depth. If double-diffusive convection were absent then the data points would fall on the mixing line which joins the point in $(\alpha T, \sigma)$-space representing the original tank fluid (OTF) with the source fluid point. The theory of Baines & Turner allows us to calculate the step in properties which occurs at the first front (e.g. our equation (7)), and the values of αT and σ just below the first front in this experiment

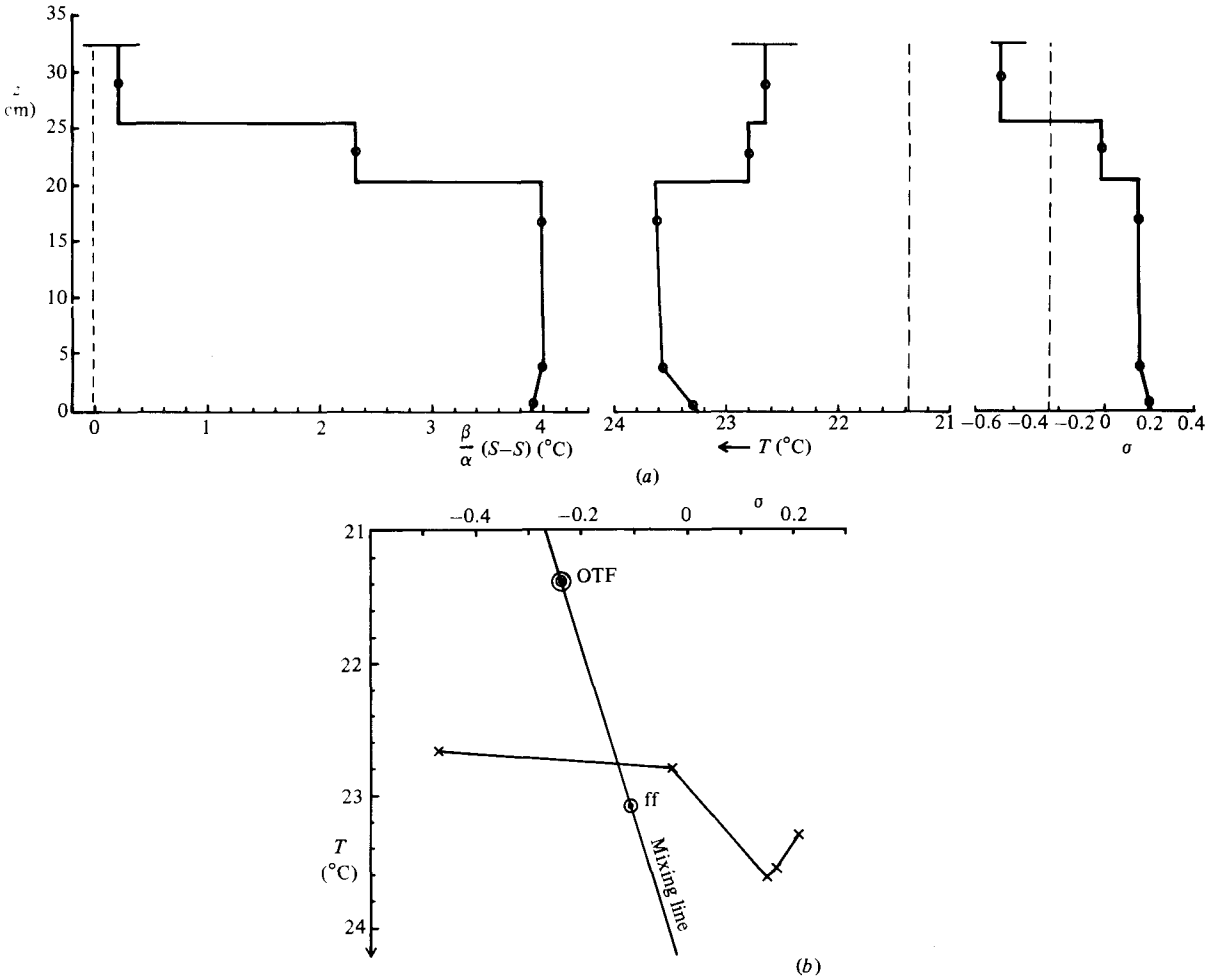

FIGURE 10. (*a*) Vertical profiles of the three properties for the heat–salt diffusive experiment. $R_\rho = 1.356$, $B_\rho = 0.14$. The data were taken 2.25 h into the experiment. Note that the units of $\beta(S-S_0)/\alpha$ (where S_0 is the initial salinity of the tank) are °C. The typical filling-box timescale t_{fb} was 3.5 h for this experiment. $\sigma \equiv (\rho - 1) \times 10^3$. (*b*) Graph of temperature versus density for the data of (*a*). The symbols 'OTF' and 'ff' are explained in the caption of figure 9(*b*).

are given by the point labelled ff in figure 9(*b*). The crosses are the data points of the layer properties replotted from figure 9(*a*), and the straight lines drawn between the crosses represent the change in properties at the sharp interfaces. Note that the step of αT at the first front is similar to that without double-diffusive convection, although the fluid above this level is less dense and less salty than the original tank fluid. Note also the lowermost interface marked ℓ, which is set up in the finger sense.

Figure 10 shows the corresponding data to figure 9, but now for a *heat–salt* diffusive case with the density-anomaly ratio $R_\rho = 1.356$ and $B_\rho = 0.14$. The upper two interfaces were clearly defined on the shadowgraph and so we have drawn these in as sharp interfaces in figure 10(*a*). There were no clearly defined layers near the bottom of the tank and so we have simply connected the data points together there.

3.2.3. *The movement of the interfaces in the tank*

Figure 11 shows the movement of the double-diffusive interfaces in the sugar–salt diffusive experiment with $R_\rho = 1.0118$ and $B_\rho = 0.85$. This was the most active (i.e.

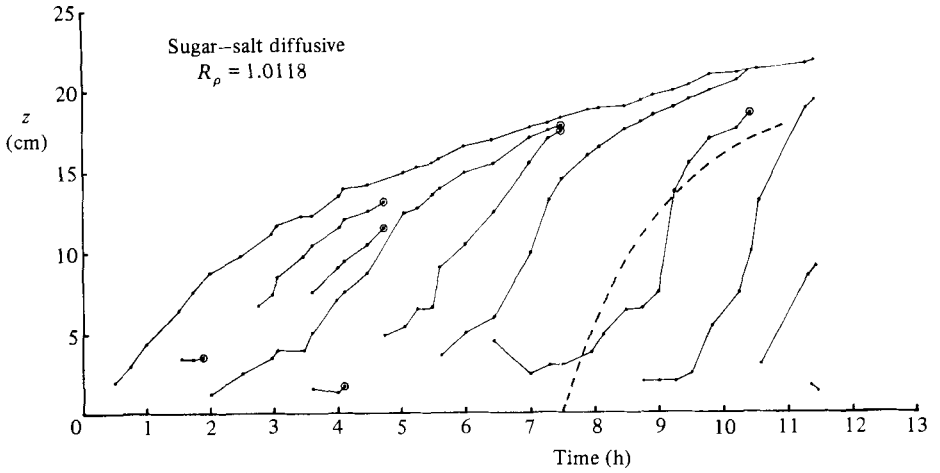

FIGURE 11. A plot of the time history of the depth z of the double-diffusive layers in the sugar–salt diffusive $R_\rho = 1.0118$ experiment. The rise velocity of the first front is given by the uppermost line. A circle at the end of an interface's time-history line represents the demise of this interface. Note that layers rise to the first front and then disappear, so increasing the contrast in properties across the first front. The typical filling-box timescale was 5.2 h for this experiment.

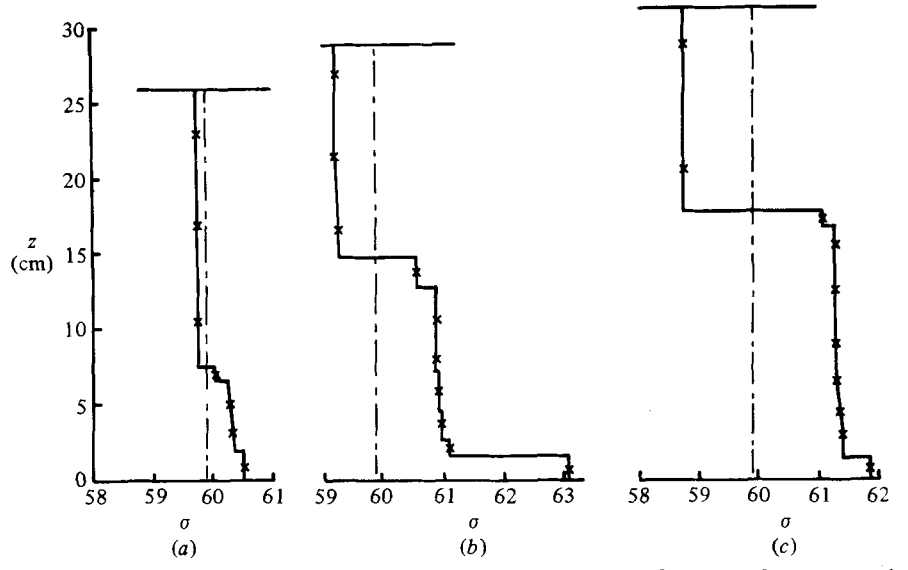

FIGURE 12. Density profile taken at 2 h (*a*), 5.75 h (*b*) and 9 h (*c*) in the sugar–salt diffusive $R_\rho = 1.0118$ experiment. The source is at a height of 25 cm. The dashed line shows the density of the original tank fluid. The filling-box timescale t_{fb} was 5.2 h in this experiment. $\sigma \equiv (\rho - 1) \times 10^3$.

the highest value of B_ρ) experiment we conducted in the diffusive sense. Note that the interfaces rise with time until they almost reach the first front. Then they disappear and their contrast in properties is added to that across the first front. In this way, the steps of T, S and σ across the first front increase (intermittently) with time. The slope of the dashed line in figure 11 is the vertical rise velocity of a layer given by the filling-box model of Baines & Turner in the asymptotic (i.e. long-time) regime. When the rise velocity of an interface in our experiments is less than that of their model we can understand this as being due to some of the plume fluid flowing

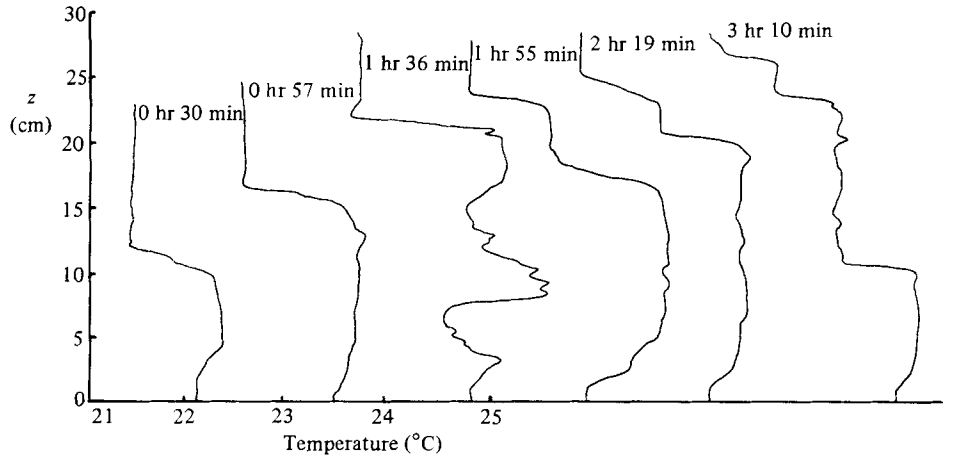

FIGURE 13. Temperature profiles at approximately 30 min intervals during a heat–salt diffusive experiment with $R_\rho = 1.356$, $B_\rho = 0.16$, $t_{fb} = 3.5$ h. The temperature scale is not quite linear. Each profile is shifted to the right by the distance on the temperature scale between 21 °C and 22 °C.

out into the environment above this interface. When the rise velocity is greater than the filling-box model predicts, this must be due to transient horizontal non-uniformities in the tank. The density profiles taken at 2 h, 5.75 h and 9 h during this same experiment (shown in figure 12) show an increasing density step at the first front and relatively little density structure below this level in the second and third profiles.

The six temperature profiles shown in figure 13 demonstrate the variability of the depth at which the plume discharges into the environment. Note that between 57 min and 1 h 36 min the fluid at a height of 7 cm has not changed much in temperature, but significant amounts of warming have occurred both above and below this level. Also a comparison between the profiles at 2 h 19 min and 3 h 10 min shows that the plume fluid spread out at heights less than 10 cm during this time interval.

The general picture which emerges is of a series of interfaces which tend to rise through the tank; this cannot however be interpreted as implying that the plume constantly spreads out at the bottom of the tank. Rather, the height of spreading of the plume is variable and no consistent pattern in this variation was apparent.

3.2.4. *Experimental measurements of D_ρ*

Finally we present a plot of D_ρ as a function of B_ρ. The parameter D_ρ is a depth-averaged measure of the (time-integrated) fluxes of buoyancy caused by double-diffusive convection normalized by the total input of buoyancy due to the filling-box process. D_ρ is determined from the measured density profiles. On the other hand, B_ρ is the theoretical parameter which represents the ratio of the typical rate of change of density in the tank due to double-diffusive convection to that due to the filling-box process, and it is derived using the property contrasts across the first front. Because of the similarity in the definitions of B_ρ and D_ρ (both involve density changes in the tank due to the two physical processes present) it is encouraging to obtain a good correlation between them in figure 14. The straight lines in figures 14 (*a*) and (*b*) are drawn with a slope of 1 and so imply direct proportionality between D_ρ and B_ρ. The datum point in figure 14 (*a*) at the smallest value of B_ρ has very large relative error bars because the densities did not change very much by double-diffusive

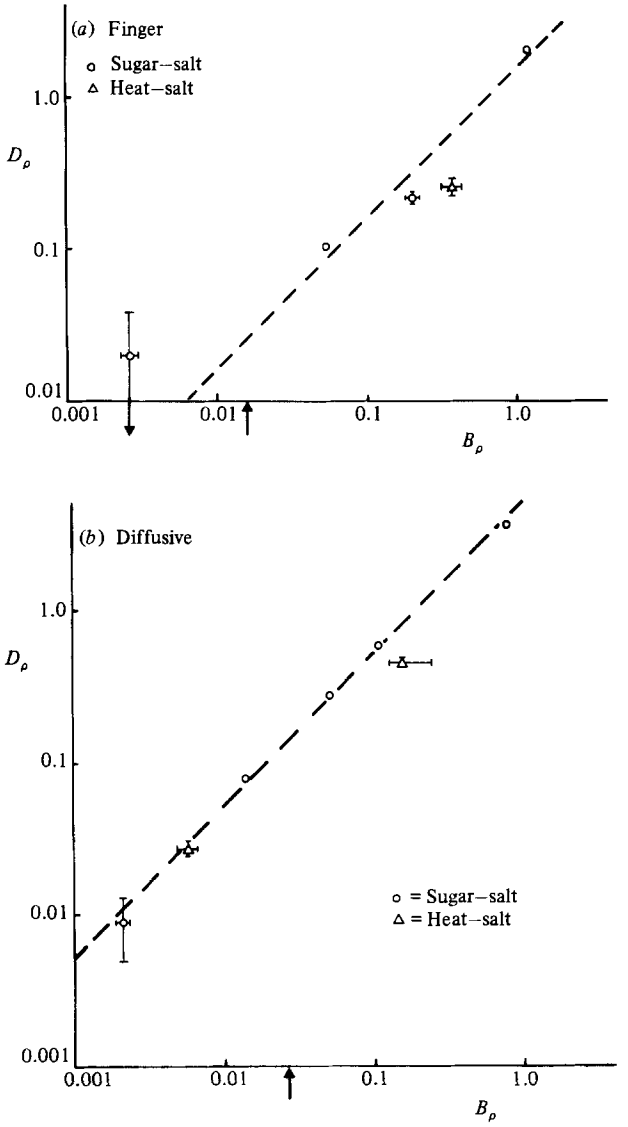

FIGURE 14. Plots of the experimentally determined density distribution parameter D_ρ as a function of the theoretical parameter B_ρ for the finger experiments (*a*) and the diffusive experiments (*b*).

convection. The fact that the data points for the heat–salt cases in figure 14 agree reasonably well with the sugar–salt data gives further confidence in the accuracy of the published laboratory flux laws for the four different cases. The critical value of B_ρ which, if exceeded, leads to lift-off is indicated in figures 14(*a*, *b*) by the arrows on the abscissae. This critical number is only known approximately, and it was determined simply by taking the average of the largest value of B_ρ in our experiments for which lift-off did not occur and the next larger value of B_ρ for which lift-off was observed.

The density profiles which were used to evaluate D_ρ in figure 14 were taken at times t such that t/t_{fb} was between 1.3 and 2.5 for all the sugar–salt experiments. The data for the heat–salt cases were taken near $t/t_{\mathrm{fb}} = 0.7$. So far we have not dwelt on how

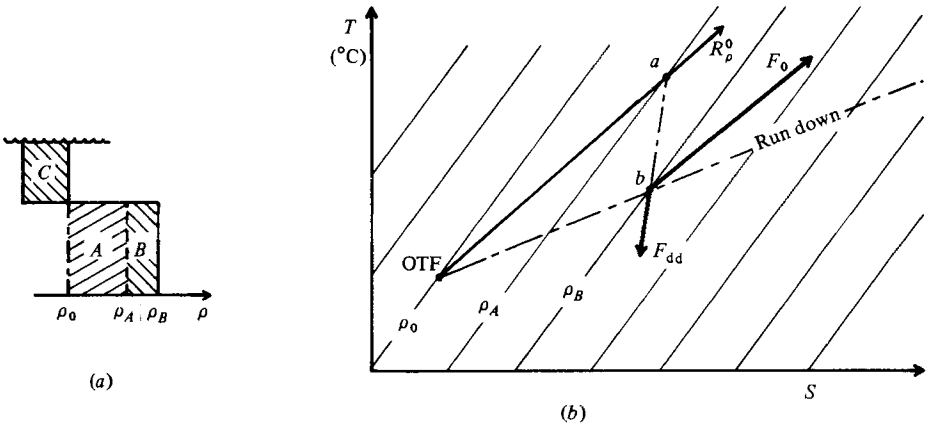

FIGURE 15. (*a*) shows a simplified density profile at times much greater than the filling-box timescale t_{fb}. ρ_A is the density in the absence of double-diffusive convection. In terms of the areas of this sketch $D_\rho = \frac{1}{2}(B+C)/A$. (*b*) is a (T, S)-diagram for the heat–salt diffusive case. OTF represents the temperature and salinity of the original tank fluid, and the filling-box process alone causes the properties below the first front to move out along the line labelled R_ρ^0.

the characteristics of the double-diffusive filling-box system may change with time, but in presenting the data of figure 14 we have implicitly assumed that D_ρ reaches a 'steady-state' value after a sufficiently long time. We discuss this proposition here.

In the single-component filling-box model with an ideal source of buoyancy, the density gradient below the nozzle approaches a steady state and the density itself increases linearly with time. In the present case where double-diffusive convection is present, there is also a flux of buoyancy across the first front. This buoyancy flux increases with the growing property contrasts across the first front. How then can we reasonably expect that our density distribution parameter D_ρ will not change appreciably for times greater than the filling-box timescale t_{fb}? Figure 15 displays the basis for this argument. We consider times greater than t_{fb} and make the simplifying assumption that the properties below the first front are uniform. Figure 15(*a*) shows the density profiles both with and without double-diffusive convection. D_ρ is given in terms of the areas in figure 15(*a*) by $\frac{1}{2}(B+C)/A$, and since $B = C$ we have

$$D_\rho = \frac{B}{A} = \frac{\rho_B - \rho_A}{\rho_A - \rho_0}. \tag{15}$$

In the absence of double-diffusive convection, an ideal source of buoyancy F_0 causes the fluid properties T, S and ρ to move out along the line marked R_ρ^0 in figure 15(*b*) and at a certain time the point a is reached. Now double-diffusive convection causes properties to change in the ratio of the buoyancy-flux ratio R_f and this is given by the slope of the F_{dd} vector. The intensity of double-diffusive convection across a sharp interface is very sensitive to the density-anomaly ratio R_ρ at the interface, and the activity tends to virtually cease for a moderately large R_ρ. When the upper layer is very deep so that its properties remain virtually unchanged at the OTF values, R_ρ is the reciprocal of the slope of the line on figure 15(*b*) joining OTF to the particular point representing the layer properties (point *b*). The R_ρ on the line marked 'run down' is then larger than R_ρ^0, and the strength of the double-diffusive convection (given by the length of the F_{dd} vector in comparison with the length of the F_0 vector) is less at point *b* than it would be at point *a*. Now, from the geometry of figure 15(*b*) it is

apparent that D_ρ (given by (15)) is constant on the line of constant R_ρ marked 'run down'.

Our argument for the approximate constancy of D_ρ for $t > t_{fb}$ rests on the sensitivity of double-diffusive convection to R_ρ, and we propose that at each time the system runs down to an approximately constant value of R_ρ. The locus of the point b which represents the (uniform) properties below the first front moves by the vector addition of the F_0 and F_{dd} vectors, and by the constant-R_ρ assumption it proceeds along the 'run-down' line in figure 15(*b*), thereby achieving a constant D_ρ. A similar but geometrically more complicated argument can be made for the approximate constancy of D_ρ for $t > t_{fb}$ when the upper-layer depth is not large. We conducted only one experiment for long enough to test this hypothesis. This was the sugar–salt diffusive experiment with $R_\rho^0 = 1.0118$, and here we compare the data taken at 5.75 h ($t/t_{fb} = 1.1$), which gave $D_\rho = 3.35$, with that taken at 9 h ($t/t_{fb} = 1.73$), which gave $D_\rho = 3.62$. This is heartening agreement.

We also believe that this independence of time (for $t \gg t_{fb}$) also applies to the question of whether 'lift-off' will or will not occur. Once the experiment has been running for several filling-box timescales, the first front has risen almost to the source of buoyancy. Little fluid is then entrained into the plume from above the first front, and so the processes which determine the density gradient below the first front will not change after this time. If lift-off has not occurred within a few filling-box timescales then it is unlikely to occur at later times.

4. Discussion

So far we have discussed the effects of double-diffusive convection in the plume itself (§2) and in the environment (§3) quite separately. By way of comparison between these processes we consider a specific example with a volume flow rate from the source of say 10 cm^3 s^{-1} and a temperature difference of 10 °C. In order for double-diffusive convection to be important in the plume, $\mathscr{R}$ needs to be less than 2×10^4, and using the values for Q and ΔT above this means that the density difference between the plume and the environment must be less than 0.5×10^{-3} g cm^{-3}, or equivalently the density-anomaly ratio R_ρ must be less than 1.15. This is quite a small value of R_ρ, and care is required in the laboratory to achieve density differences as small as this. On the other hand, the parameter B_ρ, which has to exceed a value like 10^{-2} for double-diffusive convection to be important in the filling-box geometry, contains the geometrical factors of area A and depth H, which can vary quite independently of the properties of the source of buoyancy. In this way, a given buoyancy source with a reasonably large R_ρ can give rise to significant double-diffusive effects when it flows into a tank with a large enough horizontal area, and so we may regard the conditions necessary for double-diffusive convection in the plume itself as rather more special than those required for double-diffusive convection to be important in a filling-box experiment.

We return now to discuss in more detail two of the applications of this work. Firstly we consider the production of warm salty bottom water in the ocean 70 million years ago. We assume that the present-day buoyancy flux F_0 of cold saline water from the Weddell Sea is of the correct order of magnitude for the buoyancy flux of warm saline water in the past. The volume flux of source water from the Weddell Sea is taken from Warren (1981) as 2×10^6 m^3 s^{-1} and a typical buoyancy difference $g\Delta\rho/\rho_0$ as 5×10^{-4} m s^{-2}, giving an estimate for F_0 of 10^3 m^4 s^{-3}. A suitable value of R_ρ for the warm salty bottom water formation is difficult to estimate, and we shall merely use

$R_\rho = 2$. We take the depth of the ocean as 5 km and the area A of the world ocean as 3×10^8 km^2. Substituting these values into (11a), we find a value for the parameter B_ρ of about 3000, and so we expect that double-diffusive convection will be very important in this situation. It will not, however, be an easy task to combine the double-diffusive nature of this process with fluxes through the water column caused by intermittent turbulence, which is traditionally parameterized with a diffusion coefficient. Schmitt (1981) and Schmitt & Evans (1978) have compared finger double-diffusive convection and turbulent diffusion in the present-day North Atlantic water column, and the subject obviously deserves the continued attention of oceanographers.

Secondly, we discuss at a little greater length the application to the formation of massive sulphide deposits. When a dense source of hot saline solution flows into a submarine depression of the sea floor from above, the ideas in this paper will be appropriate for a few filling-box timescales (a few t_{fb}). After the source has been flowing for such a long time that the total volume Qt discharged from the source is larger than the volume of the submarine depression, the character of the flow changes. After a sufficiently large time a steady-state balance is achieved between the incoming fluxes of heat and salt from the source and the double-diffusive fluxes of heat and salt between the fluid in the depression and the sea water above. The fluid-dynamical processes that operate in this limit of very large time will be the subject of another paper.

I wish to thank Derek Corrigan for assistance with the laboratory experiments and for the use of his aquarium tank in which the experiments of §3 were conducted. Thanks are also due to Beryl Palmer and Ross Wylde-Browne for typing the manuscript and drafting the figures respectively.

REFERENCES

BAINES, W. D. & TURNER, J. S. 1969 Turbulent buoyant convection from a source in a confined region. *J. Fluid Mech.* **37**, 51–80.

BRASS, G. W., HAY, W. W., HOLSTER, W. T., PETERSON, W. H., SALTZMAN, E., SLOAN II, J. L. & SOUTHAM, J. R. 1981 Ocean circulation, plate tectonics and climate. In *NRL Rep. on Pre-Pleistocene Climate.* In press.

GERMELES, A. E. 1975 Forced plumes and mixing of liquids in tanks. *J. Fluid Mech.* **71**, 601–623.

GRIFFITHS, R. W. & RUDDICK, B. R. 1980 Accurate fluxes across a salt–sugar finger interface deduced from direct density measurements. *J. Fluid Mech.* **99**, 85–95.

HUPPERT, H. E. 1971 On the stability of a series of double diffusive layers. *Deep-Sea Res.* **18**, 1005–1021.

HUPPERT, H. E. & SPARKS, R. S. J. 1980 The fluid dynamics of a basaltic magma chamber replenished by influx of hot, dense ultrabasic magma. *Contrib. Mineral. Petrol.* **75**, 279–289.

HUPPERT, H. E. & TURNER, J. S. 1981 A laboratory model of a replenished magma chamber. *Earth Planet. Sci. Lett.* **54**, 144–152.

KILLWORTH, P. D. & TURNER, J. S. 1982 Plumes with time-varying buoyancy in a confined region. *Geophys. Astrophys. Fluid Dyn.* **20**, 265–291.

MCDOUGALL, T. J. 1981 Double-diffusive convection with a nonlinear equation of state. II. Laboratory experiments and their interpretation. *Prog. Oceanogr.* **10**, 91–121.

MANINS, P. C. 1979 Turbulent buoyant convection from a source in a confined region. *J. Fluid Mech.* **91**, 765–781.

PETERSON, W. H. 1982 On the interaction of multiple buoyancy sources in a simple steady-state convection model. I. Submitted to *J. Fluid Mech.*

RUDDICK, B. R. & SHIRTCLIFFE, T. G. L. 1979 Data for double-diffusers: physical properties of aqueous salt–sugar solutions. *Deep-Sea Res.* **26**, 775–787.

SARSTEN, J. A. 1972 LNG stratification and roll-over. *Pipeline & Gas J.* **199**, 37–39.

SCHMITT, R. W. 1979 Flux measurements on salt fingers at an interface. *J. Mar. Res.* **37**, 419–436.

SCHMITT, R. W. 1981 Form of the temperature–salinity relationship in the central water: evidence for double-diffusive mixing. *J. Phys. Oceanogr.* **11**, 1015–1026.

SCHMITT, R. W. & EVANS, D. L. 1978 An estimate of the vertical mixing due to salt fingers based on observations in the North Atlantic Central Water. *J. Geophys. Res.* **83**, 2913–2919.

SHIRTCLIFFE, T. G. L. 1973 Transport and profile measurements of the diffusive interface in double-diffusive convection with similar diffusivities. *J. Fluid Mech.* **57**, 27–43.

TURNER, J. S. 1966 Jets and plumes with negative or reversing buoyancy. *J. Fluid Mech.* **26**, 779–792.

TURNER, J. S. 1973 *Buoyancy Effects in Fluids.* Cambridge University Press.

TURNER, J. S. & CHEN, C. F. 1974 Two-dimensional effects in double-diffusive convection. *J. Fluid Mech.* **63**, 577–592.

TURNER, J. S. & GUSTAFSON, L. B. 1978 The flow of hot saline solutions from vents in the sea floor – some implications for exhalative massive sulphide and other ore deposits. *Econ. Geol.* **73**, 1082–1100.

TURNER, J. S. & GUSTAFSON, L. B. 1981 Fluid motions and compositional gradients produced by crystallization or melting at vertical boundaries. *J. Volcan. Geotherm. Res.* **11**, 93–125.

WARREN, B. A. 1981 Deep circulation of the world ocean. in *Evolution of Physical Oceanography* (ed. B. A. Warren & C. Wunsch). M.I.T. Press.